

Chapter 5

**Particle Sizes of Casein Submicelles
and Purified κ -Casein****Comparisons of Dynamic Light Scattering
and Electron Microscopy with Predictive Three-Dimensional
Molecular Models**

H. M. Farrell, Jr.¹, P. H. Cooke¹, G. King¹, P. D. Hoagland¹,
M. L. Groves¹, T. F. Kumosinski¹, and B. Chu²

¹Eastern Regional Research Center, Agricultural Research Service,
U.S. Department of Agriculture, 600 East Mermaid Lane,
Wyndmoor, PA 19038

²Department of Chemistry, State University of New York
at Stony Brook, Long Island, NY 11794

The colloidal complexes of skim milk, the casein micelles, are thought to be composed of spherical submicellar aggregates which are the result of protein-protein interactions. Studies on submicellar particles will help to elucidate the overall structure and function of these colloidal particles. Dynamic light scattering (DLS) studies on caseinate solutions in a Pipes-KCl buffer at pH 6.75 and in the absence of calcium ions showed a bimodal distribution with comparable scattering intensity contributions using the CONTIN method of analysis. Based on the weight fraction of submicelles and that of the aggregates, the casein solution is overwhelmingly in the submicellar form with radii in the 10 nm range. Similar results were obtained for purified κ -casein, the protein responsible for colloid stability; its weight average radius was found to be 12 nm. Electron microscopy (EM) using uranyl acetate-negative staining showed that both whole caseinate and κ -casein occur as irregular spherical particles and the number average sizes for their radii in this buffer were 7.7 and 8.8 nm, respectively, which are in agreement with DLS data. To develop a molecular basis for the reasons why these two different groups of particles appear so similar, the EM data were compared with previously developed three dimensional molecular models for submicellar caseinate and κ -casein. Good correlations for the shapes and sizes of these casein aggregates can be drawn from the models and structural alterations may be predicted for generation of new functional properties.

Casein constitutes the main protein component in milk and forms stable colloidal particles of approximately spherical shape, known as casein micelles which consist of about 93% protein and 7% inorganic material (principally calcium and phosphate). Four major proteins (α_{s1} -, α_{s2} -, β - and κ -casein) are present in the

micelles of bovine milk; among these phosphoproteins, the α_{s1} -, α_{s2} -, and β -caseins are sensitive to calcium ions and become insoluble at the calcium levels encountered in milk (1, 2, 3). κ -Casein is of particular interest as it remains stable at calcium concentrations up to 400 mM and can (through protein-protein interactions), stabilize the other calcium-sensitive casein components against coagulation. The κ -casein fraction is also unique in that because of its disulfide bonding pattern, it forms stable polymers within whole casein which range from dimers to octamers and above (4).

The native casein micelles are polydisperse in size, usually ranging in diameter from 100 nm to ~600 nm in bovine milk. It is believed that casein micelles are composed of a large number of subunits (submicelles) with diameters of 10-20 nm, held together by the colloidal calcium phosphate (1, 5). The exact supramolecular structure of the casein micelle is not yet clear, although various models have been proposed ranging from a structure consisting of discrete subunits to a more or less homogeneous sphere surrounded by a hairy surface layer, to the porous gellike structure (for a recent review, see reference 2)

The self-association behavior of the individual calcium sensitive casein components in aqueous solution has been well studied (5). Reduced (SH) κ -casein has been thought to exhibit soaplike micellization, i.e. follows a monomer-micelle model (6). The self association of κ -casein is somewhat insensitive to temperature and yields a complex with an average aggregation number of about 30 and a radius of 11 nm (6). κ -Casein polymers formed in the presence of reducing agents, have a high specific volume (6.5 or 5.7 ml/g calculated from the intrinsic viscosity or the sedimentation coefficient, respectively). To accommodate the high hydration and aggregation number, a model consisting of a κ -casein shell and a hollow core has been proposed (6, 7). Two contrasting models have been introduced, one for unreduced κ -casein micelles in a simulated milk ultrafiltrate by Thurn et al. (8) and one for reduced κ -casein by deKruif and May (9). All of these models differ somewhat from those derived from earlier electron microscopy studies of κ -casein (10, 11). Because of differences in methods of preparation, the degree of disulfide bonding could influence κ -casein structure, and also the properties of whole caseins as well-a result of the central importance of the κ -casein to the whole system (1-3).

It is known that the caseins not only exhibit self-association, but also interact with each other to form associated structures. The association between the different caseins which governs the physico-chemical behavior and the size of the submicelles formed appears to be not in a fixed stoichiometric manner with respect to the four individual caseins involved, meaning that submicelles of variable composition can be formed. However, small-angle X-ray studies (12) and gel permeation chromatography experiments (13) show that the overall sizes and shapes of submicellar whole caseinates may be somewhat similar to those reported for purified κ -caseins (7, 8, 9). The present study compares the overall physical properties of sodium caseinates and κ -casein as determined by light scattering and electron microscopy with three dimensional models (14, 15) to develop a molecular basis for the divergent aggregations which apparently converge to similar particle sizes and properties.

Methods And Materials

Materials. Whole casein typed α_{s1} -BB, β -AA, κ -AA was prepared as previously described (16). This procedure involves centrifugation at 100,000 g to remove

residual lipid. κ -Casein was isolated from whole casein following the method of McKenzie and Wake (7). The κ -casein was also made lipid-free by centrifugation at 100,000 g. Polyacrylamide gel electrophoresis was according to Weber and Osborn (18) with minor modifications and at 7.5% polyacrylamide.

The whole casein was reduced and alkylated (RCM) in 8M urea essentially by the method of Schechter et al. (19). Samples, however, were dialyzed exhaustively in the dark at 4°C for 3 days against distilled, deionized water. The samples were adjusted to pH 7.0, centrifuged at 20° 100,000 × g for 20 min to remove aggregated material and lyophilized. Amino acid analysis showed >96% conversion to S-carboxymethyl cysteine. Polyacrylamide gel electrophoresis confirmed the absence of polymeric κ -casein bands (4).

Solution Preparation and Methodologies for Light Scattering. The caseinate samples were dissolved in a Pipes-KCl buffer (25 mM sodium piperazine-N,N'-bis(2-ethanesulfonate), pH 6.75, containing 110 mM KCl). The solutions were stirred for 3-5 minutes and then filtered using a low protein type Millipore filter (Millex-GV) with a nominal pore size of 0.22 μ m. The casein concentrations used were in the range of 0.8 to 4.0 mg/ml.

For submicellar caseinates, a standard laboratory-built light scattering spectrometer (20) capable of both time-averaged scattered intensity and photon correlation spectroscopy measurements in an angular range of 15-140 deg was used. Intensity correlation function measurements were carried out in the self-beating mode by using a Brookhaven BI 2030AT 136-channel digital correlator. A Spectra-Physics model 165 argon ion laser operated at 488 nm was employed as the light source. All light scattering measurements were carried out at 25.0°C. The CONTIN method (21) was used for the data analysis of dynamic light scattering results.

For dynamic light scattering of κ -casein, glassware and quartz cells were cleaned with ultrapure water obtained from a Modulab Polisher HPLC Laboratory Reagent Grade Water System. Samples were prepared as described above. Dynamic light scattering was measured with a Malvern System Model 4700c equipped with a 256 channel correlator. Light at 488 nm was provided by a Spectra Physics Model 2020 5W laser. The ATTPC6300 computer supplied by Malvern was enhanced with a Sota 386si High Performance Accelerator card. Solutions were maintained at 25°C with filtered water in the goniometer chamber bath. Dynamic light scattering measurements were made at several angles using a small aperture in the photomultiplier detector. Photon count rates were kept in the low range by controlling the size of the laser beam. The data were processed by Malvern Automeasure v 4.12 software. Multi-angle analysis by Marquardt minimization was carried out with the Malvern software (22). The performance of the system and analysis software was tested on Latex Beads, 91 and 455 nm diameter (Sigma Chemical Co.).

Electron Microscopy of Caseins. Samples of whole casein, reduced carboxymethylated (RCM) whole casein and κ -casein were prepared for electron microscopy by dissolving the casein in PIPES-KCl buffer (25 mM piperazine-N,N'-bis(2-ethanesulfonic acid) pH 6.75, containing 80 mM KCl). The samples were

made up to be 30 to 35 mg/ml and were passed through 0.45 μm filters. The filtrates were adjusted to 25 mg/ml with filtered buffer. Here the starting concentrations are much larger than those used in DLS, because of the dilutions attendant to the microscopy samples. Thin support films of amorphous carbon were evaporated on strips of cleaved mica and mounted on 400 mesh copper grids. All procedures were carried out in a water bath with samples and reagents at 37°C. Aliquots (10 μL) of caseins in buffered solution were placed on freshly prepared support films and suspended for 30–60 seconds over a water bath at 37°C; then the sample-side of the grid was washed with a controlled stream of 10 to 15 drops of buffered solution from a disposable Pasteur pipette containing 1% glutaraldehyde at 37°C. This was done to physically stabilize the composition of monomers in the form of complexes and to trap the equilibrium structures, while subsequently reducing the protein concentration to produce a discontinuous monolayer of casein particles. The adsorbed κ -casein particles or submicelles were then washed with a similar controlled stream of 5 to 10 drops of 2% uranyl acetate solution at 37°C for negative staining. Excess uranyl acetate solution was absorbed from the grid surface into Whatman #1 filter paper, and grids were allowed to air dry at room temperature.

Images of caseinate structures in randomly selected fields on grids were recorded photographically, at instrumental magnifications of 88,000 \times using a Zeiss Model 10B electron microscope (Thornwood, NY) operating at 80KV, and 97,000 \times using a Philips Model CM12 scanning-transmission electron microscope (Rahway, NJ) operating at 60 KV. Photographic prints were prepared at a magnification of 442,500 \times and the circumferences of individual submicelles were traced onto transparent overlays. The overlays were digitized and circular diameters of the tracings were calculated and plotted using Imageplus software and a Dapple Microsystems digital image analyzer (Sunnyvale, CA).

Construction of Casein Aggregates by Molecular Modeling. The model κ -casein aggregate structure employed the energy minimized κ -casein model which was previously reported by this laboratory (15). Aggregates were constructed using a docking procedure on an Evans and Sutherland (St. Louis, MO) PS390 interactive computer graphics display driven by Sybyl molecular modeling software (Tripos, St. Louis, MO) on a Silicon Graphics (Mountainview, CA) W-4D35 processor. The criterion for acceptance of reasonable structures was determined by a combination of experimentally determined information and the calculation of the lowest energy for that structure. At least ten possible docking orientations were constructed, energy minimized, and assessed for the lowest energy in order to provide a reasonable sampling of conformational space.

Energy Minimization–Molecular Force Field. A full description of the concepts behind the use of the molecular force fields (including relevant equations) was given in previous communications (14, 23). In these calculations for protein-protein interactions, a Kollman Force field was employed (24). This force field uses electrostatic interactions calculated from partial charges derived by Kollman

and coworkers. The following calculations were also used: a distance dependent dielectric constant, a united atom approach with only essential hydrogens, a cutoff value of 0.8 nm for all non-bonded interactions, and a conjugate gradient technique.

RESULTS AND DISCUSSION

Size of Casein Submicelles and κ -Casein as Determined by Dynamic Light Scattering. When the non-protein phase of the native casein micelles is removed by dialysis, the disintegration of the whole micelle occurs, leading to the formation of small spherical protein complexes called submicelles which consist of α_{s1} -, α_{s2} -, β -, and κ -caseins in an approximate ratio of 4:1:4:1 (1-3). Here we report our results obtained by dynamic light scattering on the average hydrodynamic size and the distribution of characteristic relaxation rates of casein submicelles which are formed by protein-protein interactions from sodium caseinate in a Pipes buffer (pH = 6.75, 110 mM KCl) in the absence of calcium ions. The casein concentration used was 8.15×10^{-4} g/ml. Figure 1 shows the results of the CONTIN analysis of the dynamic intensity data obtained at different scattering angles and at 25°C. The most striking feature of the plots given in Figure 1 is that instead of a unimodal distribution as expected for casein submicelles from small-angle X-ray scattering (12) and gel permeation chromatography (13), a well separated bimodal distribution has been consistently observed regardless of the scattering angle used, i.e., the scale of the probe window employed. The observation that, by varying the scattering angle from 15° to 90°, the intensity ratio of the two peaks in Figure 1 was dependent only weakly on the magnitude of the scattering vector, seems to rule out the possibility that the slow component monitored was caused by any dust contaminants. As seen from Figure 1, both the fast and slow species, in particular the former, have relatively narrow polydispersity, since the corresponding normalized variances are about 0.02 and 0.10, respectively. Based on this argument we may take the average diffusion coefficient (z-average, as deduced by the CONTIN analysis) to characterize each fraction. The average fast and slow diffusion coefficients plotted as a function of squared magnitude of scattering wave vector showed that the D_f values obtained at different scattering vectors, although somewhat disperse, were randomly distributed around an average value and showed essentially no q -dependence, as justified by the fact that for the fast component the relation $qR_h \ll 1$ holds. In contrast, the slow component exhibited a mild, but noticeable q^2 -dependence, because $qR_h \geq 1$, particularly at higher scattering angles. Thus, D_f and D_s (by extrapolation to zero scattering angle) were found to be $(2.7 \pm 0.3) \times 10^{-7}$ and $(3.3 \pm 0.2) \times 10^{-8}$ cm²/s, respectively. By using the Einstein-Stokes relation (25), the corresponding R_h values were calculated to be 8.8 ± 1 nm and 74 ± 4 nm, respectively. Apparently, the fast component with a large average diffusion coefficient corresponds to the casein submicelles, thus supporting the previous observations on the submicellar size (12,13).

At the present moment we have no conclusive answer to the nature of the slow component. The question arises as to whether these larger particles are aggregates

of submicelles, or whether they are associated structures related to only some of the casein components. It is important to note that the complex formation between the four casein components yields structures (casein submicelles) having a smaller size than that of individual casein components, e.g., α_1 - and β -caseins. This means that as a result of the coexistence of all caseins in solution the complexes behave differently as compared to complexes of any single casein component. Pepper and Farrell (13) reported that for soluble whole casein in solution, changes in protein concentration may result in a variation of association behavior. For example, with increasing casein concentration the components of whole casein form submicelles. But, with decreasing casein concentration the κ -casein dissociates from the other casein components, forming associated structures independently. However, a single peak appeared on the gel chromatogram after the SS bond of κ -casein was reduced by dithiothreitol. We have performed dynamic light scattering measurements on the above casein solution in the presence of dithiothreitol (DTT). By comparing Figs. 1c (no dithiothreitol added) and 1d (the dithiothreitol concentration was 0.1 mM), no noticeable differences were detected. Finally RCM (reduced carboxymethylated) casein yielded virtually identical results (25).

As noted above the casein solution shows an angular dependence of scattered intensity which can be ascribed to the presence of the slow component. Because of its relatively large size (~75 nm radius), the intraparticle interference associated with the slow component accounts for the decrease in scattered intensity with increasing q . By correcting for interparticle interference (25) the weight fraction of each component can be estimated. Figure 2 clearly shows that the slow component does exist, but in a very small amount. Thus, the submicelles are dominating in quantity in agreement with previous findings (5, 13).

κ -Casein samples were also subjected to dynamic light scattering analysis in the same buffers as whole caseins. Samples were analyzed for particle size at 30, 60, 90 and 120°. Data analysis by the Malvern multi-angle program also showed two peaks analogous to those seen for whole casein. The results are given in Figure 3 for the weight average distribution. The smaller sized particles centering about 11.8 nm radius account for greater than 98% of the weight fraction of the material, while the larger sized particles centering about 110 nm radius account for less than 1%. Thus both whole casein and κ -casein exhibit similar bimodal particle size distributions, but the κ -casein particles are larger on the average.

Electron Microscopy of Whole Caseins. The dynamic light scattering results obtained above show that both submicellar casein and κ -casein exhibit similar overall particle size distributions. Parallel conclusions can be drawn from comparisons of gel permeation chromatography results (13). Although the overall shape of a particle can be calculated from these methods, the specific distribution of voids and surface deformations can not be detected because of the relatively low resolution of the scattering experiments which are the average structure of many particles. With this in mind, transmission electron microscopy experiments (TEM) were carried out on whole casein under submicellar conditions (absence of Ca^{2+}) and on purified κ -casein for comparison of the previously reported 3D models with

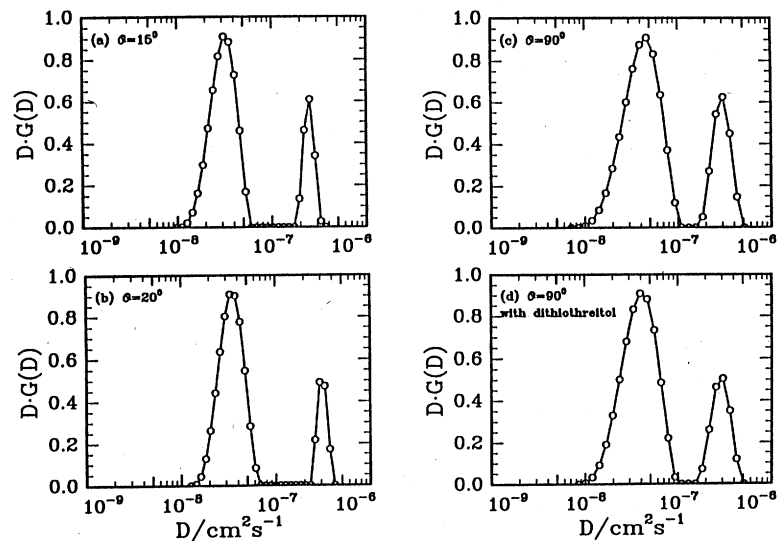


Figure 1. Relaxation rate distributions obtained at the indicated scattering angles by using the CONTIN analysis of the intensity correlation function. The peak area represents the scattered intensity contribution. (a)-(c): the whole casein solution in a Pipes-KCl buffer (pH=6.75 and total KCl=110 mM) containing no dithiothreitol. (d) the same casein solution with 0.1 mM dithiothreitol. For all solutions the casein concentration was 8.15×10^{-4} g/ml. (Reproduced with permission from reference 25. Copyright 1995 Academic.)

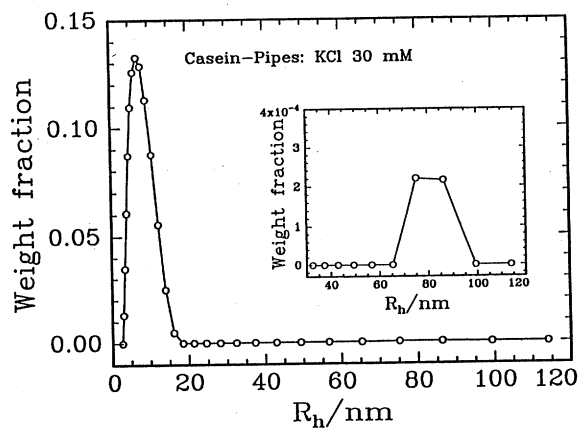


Figure 2. A plot of weight fraction distribution versus hydrodynamic radius obtained by the CONTIN analysis. The corresponding relaxation rate distribution is shown in Figure 1a. The inset shows an enlarged distribution profile for the large-size fraction. (Reproduced with permission from reference 25. Copyright 1995 Academic.)

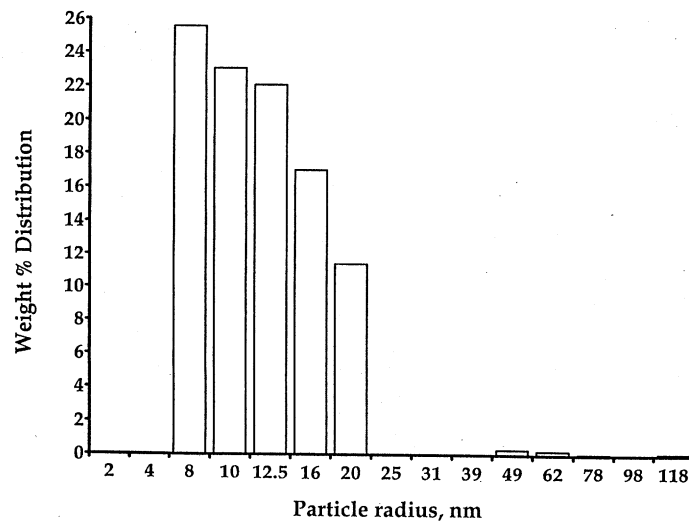


Figure 3. A plot of weight fraction distribution versus hydrodynamic radius obtained by the MALVERN analysis of κ -casein solutions. The corresponding experimental conditions are given except κ -casein in Figure 1. Concentration was 4.4×10^{-3} g/ml.

respect to predicted outlines and surface topology of the individual particles. RCM was chosen for study by electron microscopy because light scattering data showed little or no differences between native and RCM whole caseins. In addition, because the procedure for S-carboxymethyl derivatization (19) uses 8 M urea and was modified to include slow (3 day) dialysis at 4°C in the dark, a more uniform submicellar caseinate preparation with a stoichiometry of κ - α_{s1} - α_{s2} - β -casein of 1:4:1:4 for computer enhanced electron microscopy was expected.

The lyophilized RCM whole casein sample was suspended in 25 mM PIPES pH 6.75 with 80 mM KCl and processed for TEM as described in Methods and Materials. A typical example of the total field of view is shown in Figure 4. A large number of particles with diameters from 10 to 20 nm were found in agreement with the dynamic light scattering results which yielded a Stokes radius of approximately 9.0 nm for native or for RCM casein submicelles. A few larger particles, possibly due to non-fixative associated cross links, occur in the total field. When 500 particles were measured and fitted to a Gaussian function the number average radius was found to be 7.7 ± 1.4 nm. Most previous studies have indicated a cauliflower-like appearance for both micelles and submicelles, with the greatest detail for submicelles being shown in the topographical images of Kimura et al. (26). The question here is whether or not the 3D models built from the monomeric caseins (12, 14) could give rise to the observed topographical details. Procedures were devised to compare the 3D models with TEM representations at comparable scales without losing the detail of the models, but also without overextending the resolution provided by the TEM samples. The rationale behind the methods developed to make the procedure more objective has been given in detail elsewhere (27). Briefly 200 submicellar structures were selected from 6 total fields such as Figure 4, enlarged 2 \times over Figure 4, and 15 particles were selected which were thought to be similar to the predicted 3D submicellar structures by one of the authors (HMF). A montage of these 15 pictures is shown in Figure 5. The submicellar particles display at least three topographical shapes: ellipsoidal, circular and rhomboid. Selected particles of the montage of Figure 5, were then photographically enlarged to bring the scale up to low resolution images generated by the modeling graphics. To reduce the resolution of the models, van der Waals surfaces of the asymmetric 3D energy minimized submicelle structure were calculated with a density of one dot/0.01 nm², and projected on a black background. These low resolution models were used for comparison with the photographically enhanced representations of the TEM. This approach seems justified since in work with crystalline proteins whose overall dimensions are known, negative staining with uranyl salts can achieve a high TEM resolution of up to 3.0 nm (28), thus the 3D models can be considered to be of low resolution if in agreement with TEM. Particle images were analyzed by Fourier transforms and compared with particle free backgrounds. These comparisons demonstrated the maximum resolution to be at least 3 nm for all of the particles used for enhancement.

The actual 3D orientation of the submicellar particle on the thin amorphous carbon grid could not be determined so the 3D models were rotated in the computer

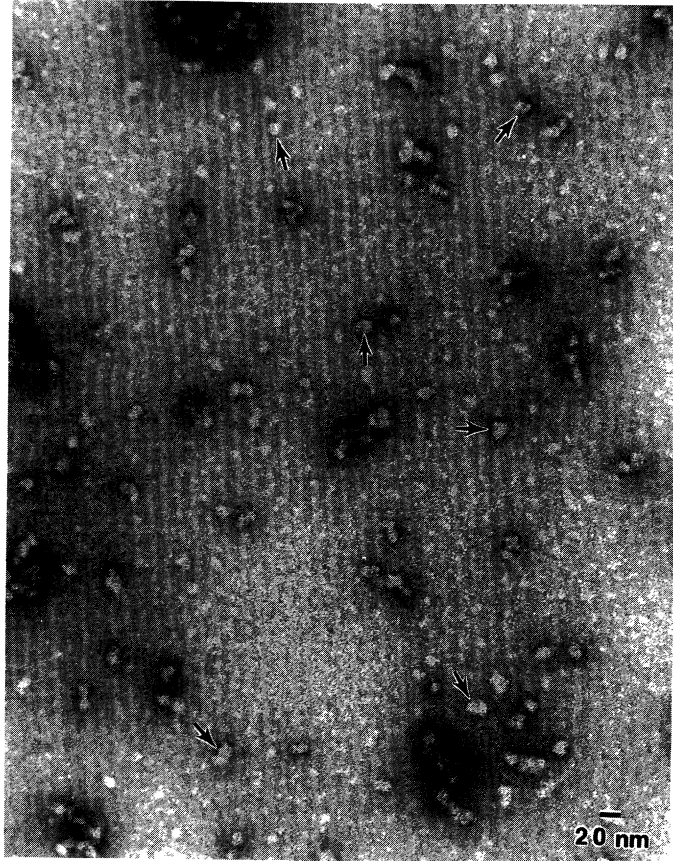


Figure 4. Negatively stained submicelles of modified whole casein. Most single particles have diameters ranging from 15-20 nm and some asymmetry in shape; bar = 20 nm.

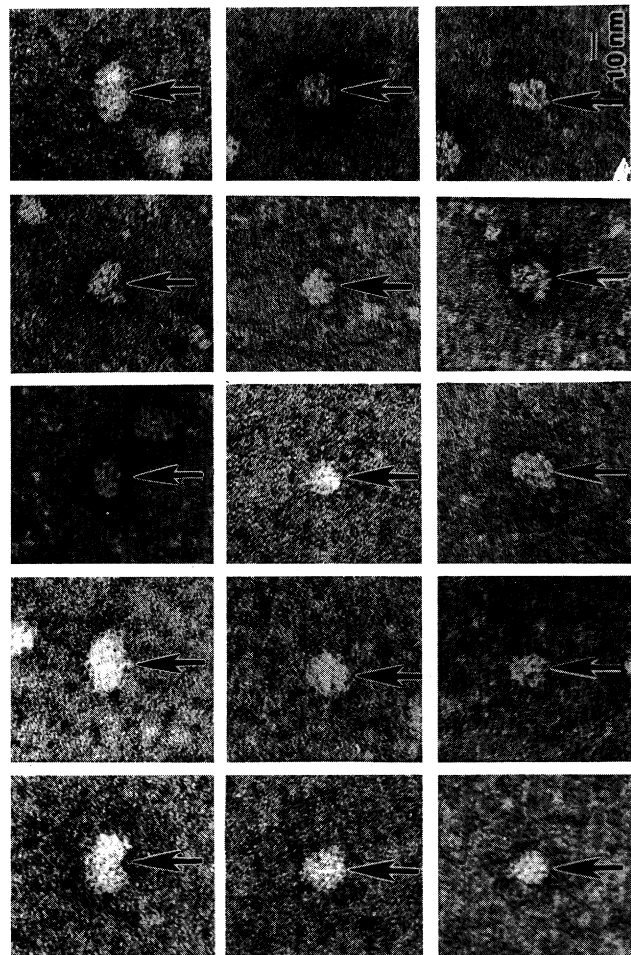


Figure 5. Selected images of submicelles, chosen from a sample of nearly 200 single particles representing three types of profiles: ellipsoidal (top row), circular (middle row) and rhomboidal (bottom row); bar = 10 nm.

for comparison with the micrographs rather than the opposite. All images compared in each TEM and 3D model are at the same scale in the figure. In Figure 6 (a) the backbone structure is shown to provide an orientation of structure in 3D space. As can be seen, this orientation of the model results in positioning of the κ -casein portion (i.e. horse and rider) at the center of the upper surface of the structure. Here the calculated van der Waals image (b) and the best representation (c) which corresponds to this bean-shaped van der Waals surface shows close agreement with respect to size, overall shape, and rugosity of surface. By rotation of this van der Waals image by 90° about the y axis (image is assumed to be in the x-y plane) the van der Waals 3D asymmetric model (d) and another TEM representation (e) are surprisingly good.

Electron Microscopy of Purified κ -Casein. When subjected to transmission electron microscopy using uranyl acetate as a negative stain, the purified κ -casein appears to occur primarily as single particles with only a few multiple particles in each field. Close examination of the micrographs shows that like whole casein, some particles have a bean-like shape and some are spherical. A typical field is shown in Figure 7. Size distributions of the κ -casein particles were made. The sample included 1500 particles from 20 fields and gave a Gaussian but narrow distribution with a number average radius of 9 nm, but greater than 86% of the particles counted gave an particle radius of 8.8 ± 0.9 nm.

Previous studies for whole κ -casein by rotary shadowing yielded diameters in the ranges of 10 to 15 nm (11) and 18 to 20 nm (10) for κ -casein particles but without statistical analysis. The particles observed in this study appear somewhat more uniform in distribution, but are in the range of the values previously reported. The rather uniform particle size observed by electron microscopy is somewhat at odds with the distribution of polymers observed for the κ -casein preparation on SDS-PAGE, in the absence of reducing agents (4). However by gel permeation chromatography these complexes are quite highly associated and in fact do not form reversible associating systems in the absence of reducing agents (13). The Stokes radius determined by gel chromatography for these maximally-associated κ -casein particles was 9.4 nm. This value is in good agreement with the average value of 8.8 nm obtained by electron microscopy in this study.

Investigations from this laboratory have generated a monomer model for κ -casein (15). This monomer model was used to assemble disulfide linked tetramers with an asymmetric arrangement of disulfides (11-88, 11-11 and 88-11). This tetrameric species is shown in Figure 8. The calculated radius of gyration for this particle is 4.7 nm which converts to a hydrodynamic radius of 6.1 nm somewhat smaller than the experimentally observed particles, and at 76,000 κ Da, smaller than the experimental molecular weight which has been reported to range from 150,000 to 600,000 (29, 30). To simulate more fully the experimental data, two structures similar to Figure 8 were docked. The octamer, whose tetramers were at a 90° angle to each other, yielded the best structure after energy minimization (-200 kcal/mole of a stabilization energy). The calculated Stokes radius for this molecule was 8.0

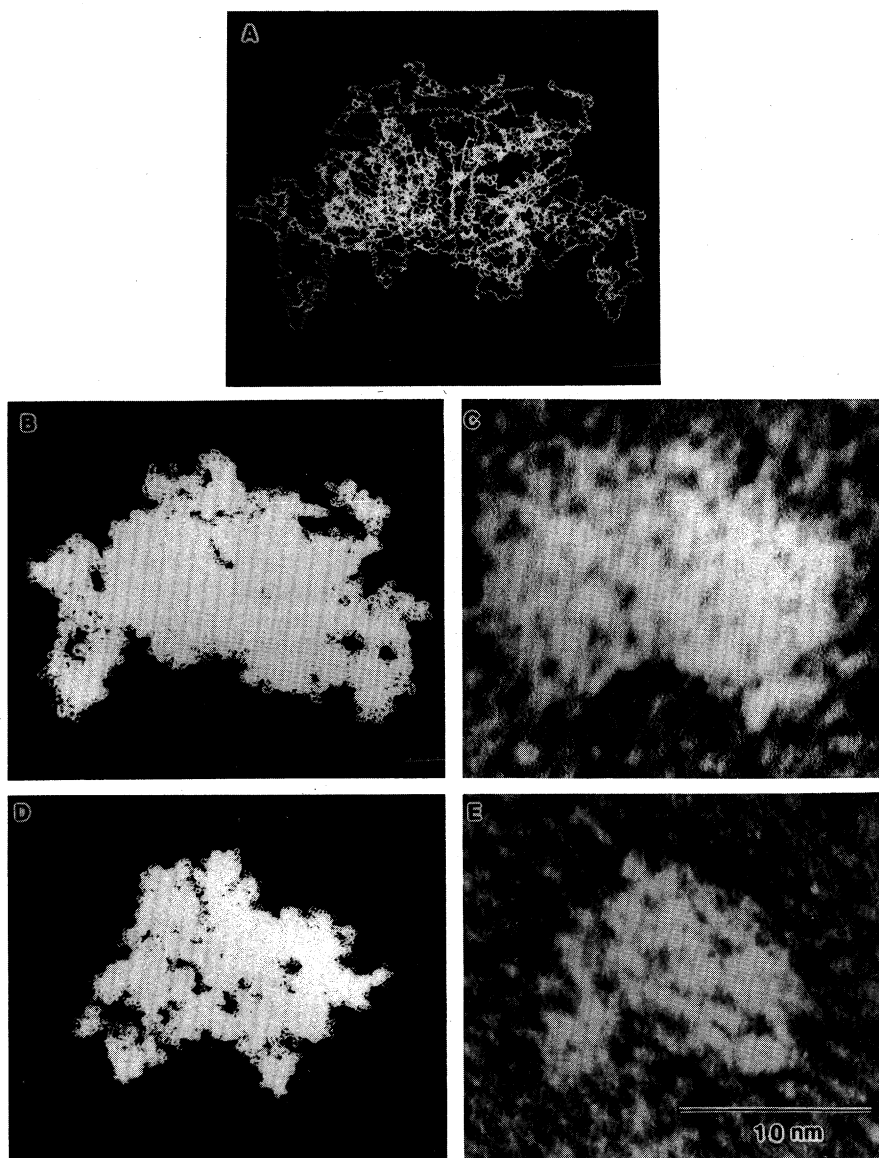


Figure 6. Comparison of matched shape and dimensions of asymmetric submicelle 3D model with photographically enlarged image enhanced representations of submicelles. (TEM bar = 10 nm; Molecular Model $\frac{1}{2}$ axis = 5nm). (A) top: backbone structure for asymmetric model; (B) left: van der Waals dot surface of model; (C) right: enlargement of image enhanced micrograph; (D) left: van der Waals of (A) rotated 90° about y axis with enlargement of image enhanced representation of the submicelle particle (E).

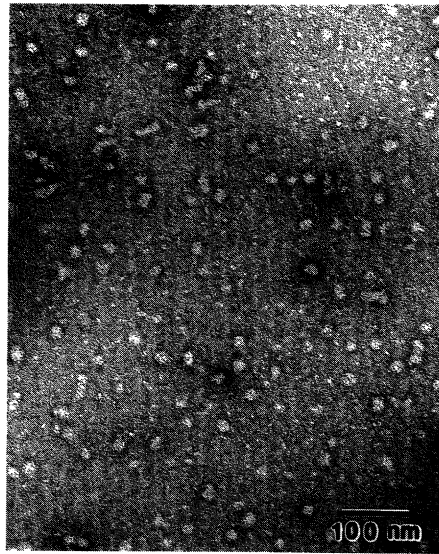


Figure 7. Transmission electron micrograph of a general field of negatively stained (uranyl acetate 2%) κ -casein.

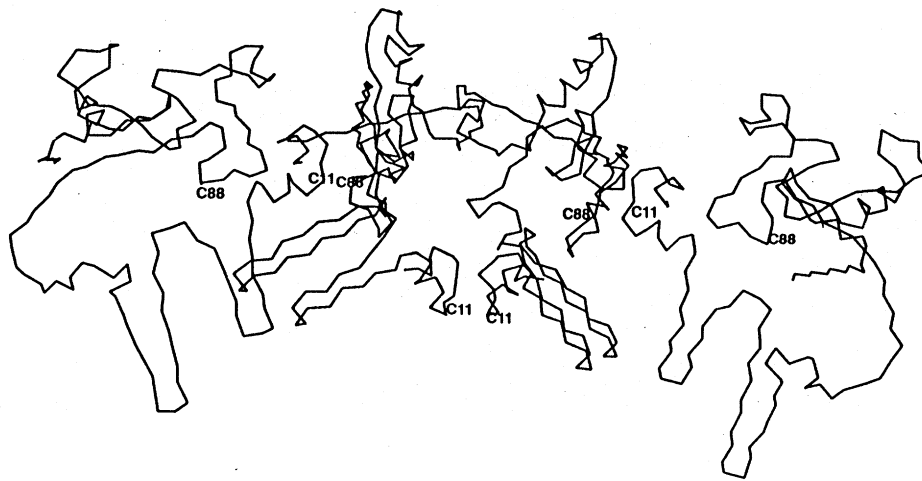


Figure 8. Three dimensional model for κ -casein tetramer linked by an asymmetric arrangement of disulfides, 11-88, 11-11, 88-11.

nm which is more in agreement with the experimental data but in the low range for aggregation number (29, 30).

The same procedures described above (Figure 6) were used for comparison of the TEM results for κ -casein to the 3D model of the octamer. Figure 9 shows the best example of the corresponding calculated van der Waals dot surface for the κ -model and best photographically enlarged TEM representations. The orientation of the upperhalf-surface of the octamer in the 3D model in space (Figure 9a) is similar to that shown in Figure 8 for the tetramer prior to docking its lower partner at 90°. The κ -casein structure exhibits surface features with long ridges 3 to 5 nm in length as found for the submicellar caseins. In addition the κ -casein 3D images on rotation (Figure 9b) may also be considered spherical as well as bean shaped (as were the submicellar images). The κ -casein 3D images still contain extended tails for the κ -casein macropeptide not visible in the TEM. It has been suggested (2) that these structures are observable hydrodynamically but are collapsed by the negative stain procedures in electron microscopy.

General Conclusions

The results obtained permit the following conclusions to be drawn for whole casein. For soluble whole casein in a Pipes-KCl buffer at pH = 6.75, DLS studies revealed a bimodal distribution either in the relaxation rate space or in the size space. The casein solution, on the weight fraction basis, remains overwhelmingly in the submicellar form with radii in the 10 nm range (8.8 ± 1 nm). RCM whole casein is in the same size range as its parent casein. RCM casein as studied by TEM has a size distribution (7.7 ± 1.4 nm) comparable to that obtained by DLS and results are compared to other studies in Table 1.

Table 1. Summary of Physical Data on Whole Caseins

	<i>M.W.</i>	<i>Radius (nm)^a</i>	<i>Method</i>	<i>Reduction</i>
Pepper (13)		9.4	GPC ^b	None
Kumosinski (12)	285,000	8.0	SAXS ^c	DTT ^d , hours
Chu (25)		8.8	DLS ^e	None
Chu (25)		8.8	DLS	RCM/DTT, hours
This Study		7.7	EM ^f	RCM

^aRadius varies by type of measurement.

^bGel permeation chromatography.

^cSmall-angle X-ray scattering.

^dDithiothreitol.

^eDynamic light scattering (weight average).

^fElectron microscopy.

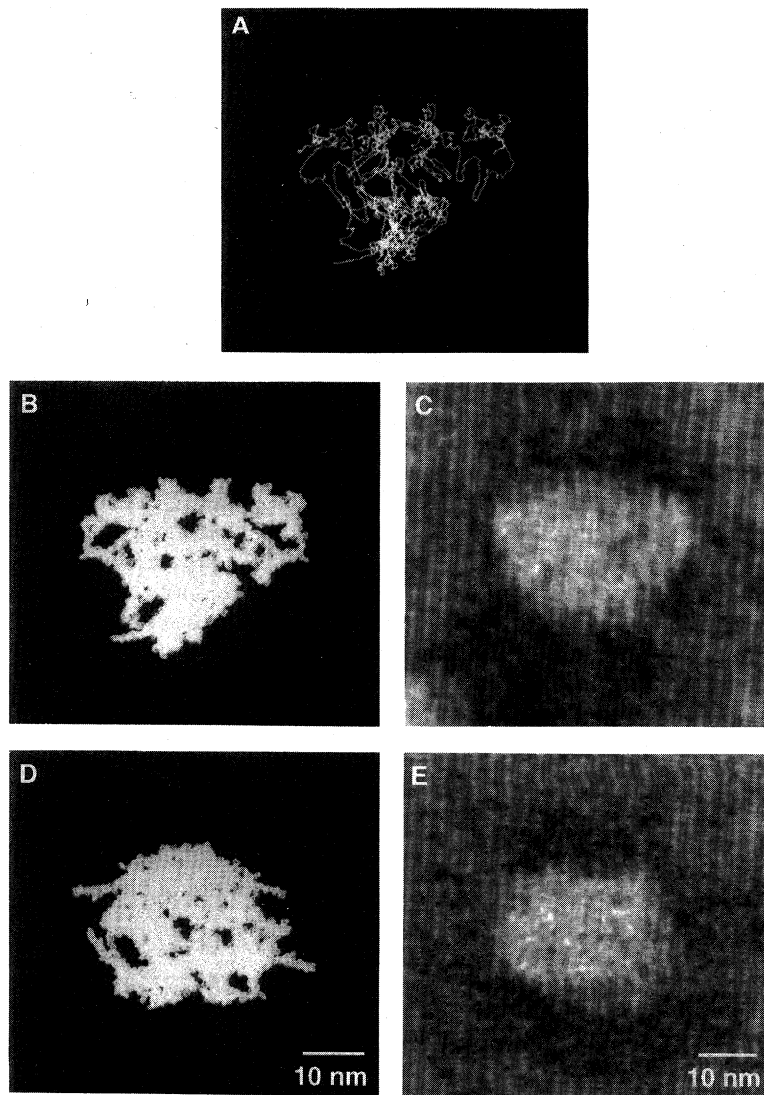


Figure 9. Comparison of κ -casein octamer 3D model after 20 psec of molecular dynamics with photographic enlargement of image enhanced representation of κ -casein. (TEM bar = 10 nm; Molecular Model bar = 10 nm). (A) Top: backbone structure for octamer of κ -casein; (B) left: calculated van der Waals surface of (A); (C) right: photographic enlargement of image enhanced EM representation of a κ -casein particle; (D) rotation of 90° about x axis of (B) van der Waals model and photographic enlargement of image enhanced EM representation of a κ -casein particle (E) showing a comparable structure.

The TEM patterns photographically enlarged are reminiscent of the surface shapes predicted by Kimura et al. (26). The results from TEM yield overall more structural information although the radii obtained for the particles are smaller than those from DLS, in line with possible stain penetration of their open porous structures.

κ -Casein, as purified from bovine milk, exhibits rather uniform distribution of particles $9.6 \text{ nm} \pm 2.5 \text{ nm}$ radius as disclosed by DLS (number average). TEM yielded a value of $8.8 \pm 0.9 \text{ nm}$. These data are at odds with some physical chemical data for κ -casein (Table 2).

Table 2. Summary of Physical Data on κ -Caseins

	<i>MW</i>	<i>Radius (nm)^a</i>	<i>Method</i>	<i>Reduction</i>
Vreeman (7)	600,000	11.1 ^b	Sedimentation	1 week, 2-ME ^c
Slattery (30)	600,000	11.2 ^d	Sedimentation	1 hour, 40 mM DTT
deKruif (9)		14.7 ^b	SANS ^e	5 mM DTT
Pepper (13)		9.4 ^d	GPC ^f	None
Thurn (8)	2,000,000	7.0 ^{b,g}	SANS ^e	None
This study		8.8 ^d	EM ^h	None
		9.6 ^d	DLS ⁱ	None

^aRadius type varies with method.

^bDEAE purified K-I casein.

^c2-Mercaptoethanol.

^dWhole κ -casein.

^eSmall-angle neutron scattering.

^fGel permeation chromatography.

^gInternal "submicellar" particle of larger aggregate.

^hElectron microscopy.

ⁱDynamic Light Scattering, number average; weight average = 11.8 nm.

It must be noted that the more recent data on the size distributions of κ -casein were not taken on the type of κ -casein used here. All of this data (7, 8, 9) was collected on samples which were reduced, purified on DEAE media in urea, dialyzed, lyophilized and then redissolved and reduced to varying extents (Table 2). The process of further isolation may yield particles with different degrees of aggregation. In this study the average radius for bovine κ -casein particles was $8.8 \pm 0.9 \text{ nm}$ which is similar to the value of 7.7 nm found for whole casein submicelles by identical electron microscopy techniques. Few higher order particles were observed in these studies. An overall view of κ -casein, as purified from bovine milk, is that of a series of disulfide-bonded polymers, ranging from monomers to octamers and above. These polymers are most likely distributed

among three possible arrangements (11-88, 88-88, and 11-11) according to Rasmussen et al. (31). The apparent heterogeneity of the individual κ -casein chains however is overcome through protein-protein interactions which yield rather uniform particles of 8.8 nm as revealed by electron microscopy or 9.6 nm by light scattering. The shape and size of the κ -casein particles are mediated in part by the rigidity of its disulfide bonds which may cause the particles to be larger than those found for both RCM and native caseins. Thus, as noted above, purification procedures may produce protein-protein interactions in κ -casein which are not present in submicellar structures; alternatively some submicelles could be pure κ -casein.

The overall size, shape and perhaps rugosity of the 3D models are in line with the photographically enlarged representations of the TEM images of both whole casein and purified κ -casein. Whether or not the porosity predicted by the 3D model occurs cannot be supported by the TEM since the depressions or pores are below resolution. Good correlation, however, between the images generated for the dot surfaces of the model and the TEM appears to exist in different spatial orientations of the models. However, when taken together with SAXS, SANS and hydration values (7, 9, 12) all of the data point toward open, highly hydrated and rugose structures for both κ - and whole caseins. The κ -casein 3D models built with a hydrophobic core and hydrophilic exterior confirm the conceptual model of deKruif and May (9) and portray internal cavities and pores necessary to accommodate the experimentally observed hydrations (6, 7).

As emphasized in previous papers on the 3D models of submicellar casein (12, 14), it must be kept in mind that these structures represent working models. They are not the final native structures but are presented to stimulate discussion and to be modified as future research unravels the nature of these non-crystallizable proteins. Inspection of a recent drawing of the casein micelle by Holt (2) demonstrates how structures such as those presented here could be further aggregated into the casein micelle. Continued dialogue and research in this area may stimulate the new concepts necessary to bring together divergent views and to finally produce an accurate micelle model. It is hoped that this work is a further step in that direction.

Literature Cited

1. Farrell, H. M., Jr., and Thompson, M. P. In *Caseins as Calcium Binding Proteins*; Thompson, M. P., Ed.; Calcium Binding Proteins; CRC Press: Boca Raton, FL, 1988, Vol. 2, pp 150.
2. Holt, C. *Advances in Protein Chem.* **1992**, *43*, 63-151.
3. Swaisgood, H. *Developments in Dairy Chem.* **1992**, *1*, 51-95.
4. Groves, M. L., Dower, H. J., and Farrell, H. M., Jr. *J. Protein Chem.* **1991**, *11*, 21-28.
5. Schmidt, D. G. In *Developments in Dairy Chemistry*, 1 Fox, P. F., Ed.; Applied Science Pub. Ltd.: Essex, England, 1982, pp 61.
6. Vreeman, H. J., Brinkhaus, J. A. and van der Spek, C. A. *Biophys. Chem.* **1981**, *14*, 185-193.

7. Vreeman, H. J., Visser, S., Slangen, C. J., and Van Riel, J. A. M. *Biochem. J.* **1986**, *240*, 87-97.
8. Thurn, A., Blanchard, W. and Niki, R. *Colloid and Polymer Sci.* **1987**, *265*, 653-666.
9. deKruif, C. G., and May, R. P. *Eur J. Biochem.* **1991**, *200*, 431-436.
10. Parry, R. M. Jr., and Carroll, R. J. *Biochim. Biophys. Acta.* **1969**, *194*, 138-150.
11. Schmidt, D. G., and Buchheim, W. *Neth. Milk Dairy J.* **1976**, *30*, 17-28.
12. Kumosinski, T. F. King, G. and Farrell, H. M., Jr. *Journal of Protein Chemistry*, **1994**, *13*, 701-714.
13. Pepper, L., and Farrell, H. M., Jr. *J. Dairy Sci.* **1982**, *65*, 2259-2266.
14. Kumosinski, T. F., King, G. and Farrell, H. M., Jr. *Journal of Protein Chemistry*, **1994**, *13*, 681-700.
15. Kumosinski, T. F., Brown, E. M., and Farrell, H. M., Jr. *J. Dairy Sci.* **1993**, *76*, 2507-2520.
16. Kakalis, L. T., Kumosinski, T. F. and Farrell, H. M., Jr. *Biophys. Chem.* **1990**, *38*, 87.
17. McKenzie, H. A., and Wake, R. G. *Biochim. Biophys. Acta.* **1961**, *47*, 240-242.
18. Weber, K., and Osborn, M. *J. Biol. Chem.* **1969**, *244*, 4406-4409.
19. Schechter, Y., Patchornik, A., and Burstein, Y. *Biochemistry* **1973**, *12*, 3407-3413.
20. Zhou, Z. and Chu, B. *J. Colloid Interface Sci.* **1988**, *126*, 171-180.
21. Provencher, S. W. *Comput. Phys. Commun.* **1982**, *27*, 119-123.
22. Cummins, P. G., and Staples, E. J. *Langmuir* **1987**, *3*, 1109-1112.
23. Kumosinski, T. F. and Farrell, H. M., Jr. In *Protein Functionality in Food System*; Chapter 2, Hettiarachy, N.S. and Ziegler, G.R., Eds.; Marcel Dekker Inc.: New York, NY, 1994, pp 39-77.
24. Kollman, P. A. *Ann Rev. Phys. Chem.* **1987**, *38*, 303-331.
25. Chu, B., Zhou, Z., Wu, G. and Farrell, H. M., Jr. *Journal of Colloid Interface Science*, **1995**, *170*, 102-112.
26. Kimura, T., Taneya, S. and Kanaya, S. *Milchwissenschaft*, **1979**, *34*, 521-524.
27. Kumosinski, T. F., Uknalis, J. J., Cooke, P. H. and Farrell, H. M. Jr. *Lebens. Wiss. Technol.* **1996**, (In press).
28. Unwin, P. N. T. *Journal of Molecular Biology*, **1975**, *98*, 235-242.
29. Swaisgood, H. E., Brunner, J. R., and Lillevik, H. A. *Biochemistry* **1964**, *3*, 1616-1623.
30. Slattey, C. W., and Evard, R. *Biochim. Biophys. Acta.* **1973**, *317*, 529-538.
31. Rasmussen, L. K., Højrup, P., and Petersen, T. E. *Eur. J. Biochem.* **1992**, *207*, 215-222.

Reprinted from ACS Symposium Series 650

Macromolecular Interactions in Food Technology

Nicholas Parris, Akio Kato, Lawrence K. Creamer, and John Pearce, Editors

Published 1996 by the American Chemical Society